Temperature Controlled Comfortable Chair For Nyctophobia And Seasonal Affective Disorders

Article *in* African Journal of Biomedical Research · January 2025

DOI: 10.53555/AJBR.v27i4S.4671

2 authors:

Harshal Ambadas Durge
Vishwakarma Institute of Technology
4 PUBLICATIONS **0** CITATIONS
SEE PROFILE

Vijay M Mane
Vishwakarma Institute of Technology
30 PUBLICATIONS **238** CITATIONS
SEE PROFILE

https://africanjournalofbiomedicalresearch.com/index.php/AJBR
Afr. J. Biomed. Res. Vol. 27(4s) (December 2024); 5721-5732
Research Article

Temperature Controlled Comfortable Chair For Nyctophobia And Seasonal Affective Disorders

Vijay Mahadev Mane[1], Harshal Ambadas Durge[2], Shital Raut[3], Siddharth Bhorge[4], Ashwini Barbadekar[5], Dr.Kalyan Devappa Bamane[6]

[1,2,3,4,5]Vishwakarma Institute of Technology, Pune, India-441037.Vijay.mane@vit.edu, harshal.durge21@vit.edu, shital.raut@vit.edu, siddharth.bhorge@vit.edu, ashwini.barbadekar@vit.edu
[6]Associate Professor, D.Y .Patil College of Engineering, Akurdi Pune-411044, kdbamane@dypcoeakurdi.ac.in

***Correspondence Author:** Vijay Mahadev Mane
*Vishwakarma Institute of Technology, Pune, India-441037.Vijay.mane@vit.edu

Abstract

Introduction: Prolonged sitting is a leading cause of discomfort, injury, and chronic pain, particularly for prehospital patients and manual wheelchair users, who are at high risk of upper-limb pain and dysfunction. These challenges necessitate the development of innovative solutions to enhance comfort, mobility, and safety for individuals with diverse medical needs.

Objectives: This study presents the development of a Temperature Controlled Comfortable Chair (TCCC), a multifunctional solution aimed at improving prolonged sitting comfort by integrating features such as temperature regulation, mobility, and safety systems.

Methods: The TCCC was designed with customizable sitting and sleeping arrangements, a temperature-regulated mattress controlled via a thermostat, joystick-controlled mobility, and an automatic lighting system. The thermostat maintained a user-specific temperature range of 26–27°C, with a warming function to aid in drying and a cooling feature to alleviate prickly heat. The lighting system, which activates at 41 lux, was implemented to enhance visibility and mitigate nyctophobia in low-light conditions. Extensive testing was conducted to evaluate the chair's ergonomic, thermal, and mobility performance.

Results: Testing revealed that the TCCC effectively maintains user comfort in various weather conditions through precise temperature regulation. The warming function demonstrated efficient drying capabilities, while the cooling function significantly reduced discomfort associated with prickly heat. The joystick-controlled mobility system provided smooth maneuverability, even with the chair's substantial weight. The automatic lighting system ensured safety and usability in low-light environments.

Conclusions: The TCCC represents a user-centric, multifunctional innovation in prolonged sitting solutions, addressing critical needs in comfort, mobility, and safety. Its ergonomic design and advanced features offer significant enhancements for individuals with medical or mobility challenges. This development underscores the importance of integrating multifunctional designs in healthcare products to advance patient care and overall user well-being.

Keywords: Comfort, Illuminance, Mobility, Patient, Temperature

Author for correspondence: Email:Vijay.mane@vit.edu*

Received:02/11/2024 Accepted: 03/12/2024

DOI: https://doi.org/10.53555/AJBR.v27i4S.4671

INTRODUCTION

Prehospital patients, particularly those with severe injuries or illnesses, are at a heightened risk of cold exposure, which can lead to hypothermia. Traditionally defined as a body core temperature below 35°C, hypothermia's definition has been revised to below 36°C due to its significant prognostic implications in trauma cases [1]. Hypothermia negatively impacts bodily functions, increasing morbidity and mortality regardless of injury severity [2]. Various factors, including fatigue, nervous system injuries, medication, alcohol, age, chronic illness, trauma, malnutrition, and endocrine disorders, disrupt the body's thermoregulatory mechanisms, leading to peripheral vasoconstriction and rapid cooling of the extremities and back [3].

Manual wheelchair users frequently encounter upper-limb pain and dysfunction, primarily due to propulsion and transfers, with up to 73% reporting chronic pain [4]. Biomechanical analyses of wheelchair propulsion have aimed to enhance mechanical efficiency and address musculoskeletal issues by investigating variables such as hand rim size, wheel camber, rim tube diameter, and seat position [5]. Despite these advances, 40% of electric wheelchair users still face maneuvering difficulties [6]. Recent research has integrated mobile robot guidance techniques into electric wheelchairs, yet challenges with joystick control persist due to physical limitations and spasticity-induced tremors [7].

Previous studies have explored the effects of seat position on wheelchair propulsion efficiency. Engel et al. determined that positioning the seat unit posteriorly relative to the rear wheels was most efficient [8]. Brubaker's findings supported this by showing that a posterior seat placement reduces rolling resistance and enhances propulsion efficiency [9]. Van der Woude et al. identified that optimal elbow flexion angles significantly affect energy consumption and kinematics [10]. Hughes et al. established a robust correlation between seat position and joint motion during propulsion, emphasizing the need for ergonomically optimal seat positioning [11]. However, these studies often focus on static configurations and fail to address the dynamic needs of users.

This study aims to develop the Temperature Controlled Comfortable Chair (TCCC), a multifunctional seating solution that integrates customizable sitting and sleeping arrangements, temperature regulation, joystick-controlled mobility, and automatic lighting. The TCCC is designed to enhance comfort, mobility, and safety for individuals with varying medical needs, addressing the limitations of previous studies by offering a dynamic and adaptable solution tailored to individual user preferences and requirements. The TCCC represents a significant advancement in ergonomic design, setting a new standard for modern seating and sleeping solutions.

OBJECTIVES

The objective of this study is to develop the Temperature Controlled Comfortable Chair (TCCC), a multifunctional seating solution integrating customizable sitting and sleeping arrangements, temperature regulation, joystick-controlled mobility, and automatic lighting. The TCCC aims to enhance comfort, mobility, and safety for individuals with diverse medical needs by addressing limitations of previous designs through a dynamic, adaptable, and user-centric approach.

METHODS

This section provides a detailed explanation of the features, as illustrated in Figure 1, and is organized into the following subsections: Proposed System, which covers circuit designs; Working, which describes the workflow of all integrated features; and Architecture, which outlines the internal and external structural views of the chair.

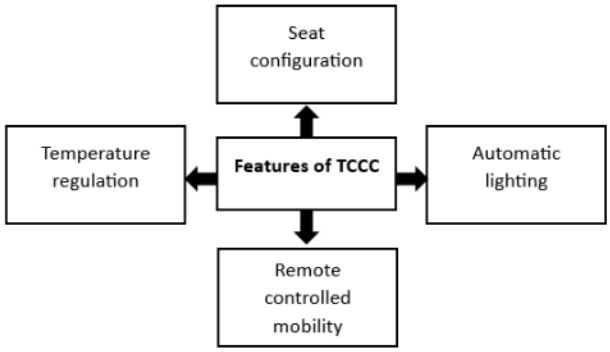

Figure 1. Features of TCCC

2.1 Proposed system

This section includes overview of 4 systems. First system is for automatic lighting, seconds for seat configuration, third system for seat temperature regulation, and fourth for remote controlled mobility. The setup involves the integration of a diverse array of components to establish a sophisticated smart seating system. At its core, an Arduino Uno serves as the central control unit, interfacing with essential peripherals including a BH1750 light sensor, servo motor, potentiometer, and relay module. These components collectively enable automatic adjustments in lighting based on ambient conditions and user-defined seating configurations. Moreover, the TCCC

incorporates dual thermostats tasked with managing a 12V DC fan and a 220V AC LED strip, pivotal for regulating seat temperatures through both warming and cooling functionalities. The chair's mobility is facilitated by an L298N motor driver module, BO motors, and a joystick interface, seamlessly integrated with the Arduino Uno. This integrated setup enables precise and remote-controlled adjustments, significantly enhancing user comfort and accessibility.

2.2 Working of TCCC

This section details the operational workflow of the four key features of the TCCC and presents the results obtained from testing.

2.2.1 Seat Configuration

Seat configuration feature leverages three servo motors to adjust the chair into various configurations for sitting or sleeping, providing ergonomic relief and addressing diverse user needs [12]. A potentiometer is used to precisely control the servo motors, enabling smooth transitions between positions [13]. The system supports multiple configurations, each tailored to a specific function. The eleven distinct chair positions depicted in Figure 2, crucial for health recovery.Different chair configurations and their corresponding purposes are defined by specific servo motor angles (θ1, θ2, θ3).

1.

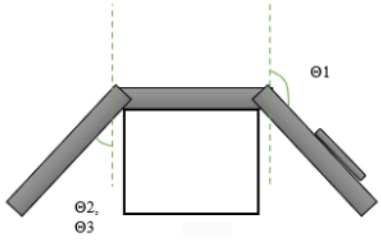

2.

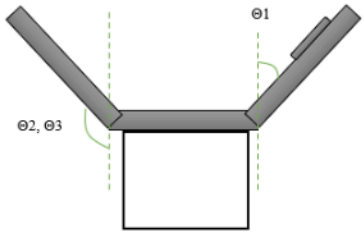

3.

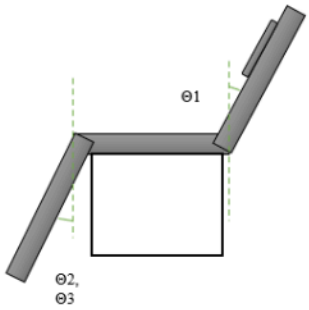

4.

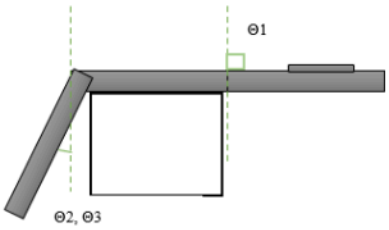

5.

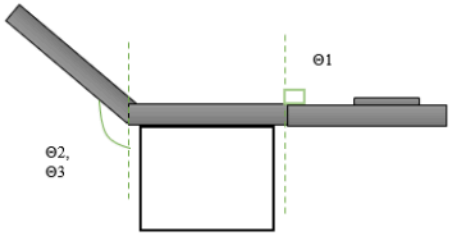

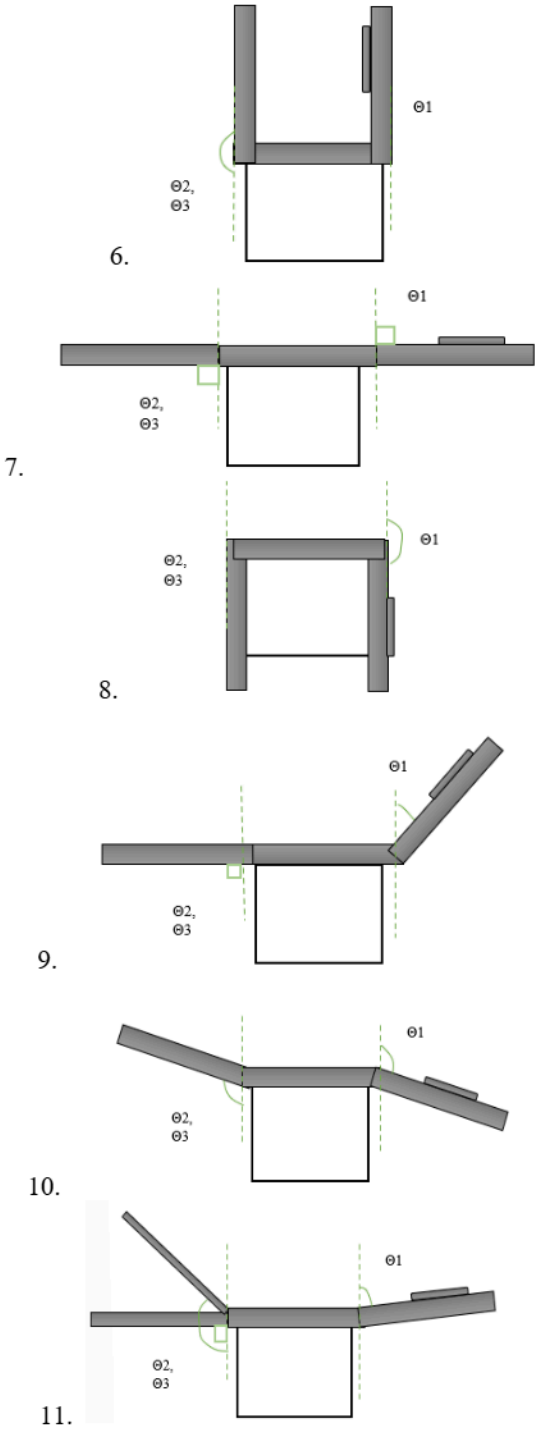

Figure 2. Seat configurations

These positions incorporate features such as abdominal exercise facilitation, relaxation promotion, and support during recovery from injury or surgery. They are designed to address various health needs, including muscle strengthening, weight loss, stress reduction, and circulatory improvement. Additionally, the configurations offer customizable seating and sleeping options, optimizing comfort, posture, and therapeutic benefits. Notably, the positions cater to diverse requirements such as leg elevation for enhanced circulation, back support for spinal alignment, and reclined postures for tension relief. Specific designs accommodate rehabilitation needs, such as aligning leg fractures and minimizing discomfort during rest and sleep.

The user adjusts the potentiometer's knob to specific angles indicated by an arrow, altering the resistance of the wiperand varying the voltage according to Equation (1).

$$V_{out} = V_{in} * \frac{R_{wiper}}{R_{total}} \quad (1)$$

where R_{total}=10k ohm

This analog voltage is converted into a digital value by the Arduino Uno's 10-bit ADC using Equation (2).

$$ADC_{value} = \frac{V_{out}}{V_{in}} * 1023 (2)$$

where V_{in}=5V
The digital value is then applied to Equation (3) to determine the corresponding servo angle, setting the servo motor's position accurately.

$$Angle = \frac{ADC_{value}}{1023} * 180 (3)$$

The obtained data is documented in table 1, which shows the corresponding wiper resistance values for specific servo angles.

Table 1. Correspondence between servo angles and wiper resistance values

Servo angle	Wiper resistance value (ohm)
0˚	0
30˚	1.67k
45˚	2.5k
75˚	4.17k
90˚	5k
120˚	6.67k
135˚	7.5k
180˚	10k

In the control section of the chair, three potentiometers are installed, each labelled with specific angles as illustrated in Figure 3. As the arrow indicates a particular angle, the servo motor adjusts accordingly to align with the corresponding angle.

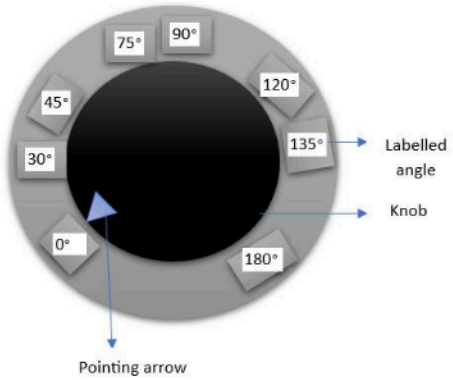

Figure 3 Potentiometer with labelled angles

Various chair configurations, including configuration number, configuration name, and the corresponding servo motor angles (θ1, θ2, θ3), along with their benefits, are defined through the use of servo motors. These configurations and their details are systematically documented in table 2.

Table 2 Seat configuration and purpose

Configuration number	Configuration name	Angle (Θ1, Θ2, Θ3)	Purpose
1	Abdominal Exercise and Weight Loss	135°, 45°, 45°	Abdominal exercise and weight loss
2	Hammock-type configuration	45°,135°, 135°	relaxation, reducing stress levels
3,4	Sitting Chairs with Adjustable Seating	30°, 30°, 30° 90°, 30°, 30°	optimal comfort and support, recovering from injury or surgery
5,6	Sleeping Positions with Leg Elevation, side supported stool type configuration	90°, 120°, 120° 0°, 180°, 180°	improve circulation, reduce swelling, and alleviate pressure on the lower back and joints and comfortable rest while minimizing strain on the spine
7	Standard Bed Configuration	90°, 90°, 90°	restful sleep and overnight recovery, supporting immune function, cognitive function, and physical recovery

8,9	Stool-type configuration, and Semi-Sleeper Seats	180°, 0°, 0° 30°, 90°, 90°	sit comfortably without putting undue pressure on the spine or lower back, relieve tension, and promote relaxation
10	Lazy Sleeping Position	120°, 120°, 120°	maintaining body balance and reducing strain on muscles and joints
11	Leg Fracture Recovery Position	75°, 90°, 135°	recovering from leg fractures,adjusting the leg portion of the seat facilitates proper alignment and support

2.2.2 Seat temperature regulation

The Temperature Controlled Comfortable Chair features a sophisticated system designed to adapt to seasonal temperature variations, utilizing two XH-W3001 thermostat modules with separate power supplies to regulate seat temperature for winter, rainy, and summer conditions [14]-[15].

The XH-W3001 220V AC thermostat is the central device for temperature control, incorporating an integrated relay to manage an LED strip's operation. Operating on a 220V AC power source, the module uses an embedded temperature sensor to monitor the current temperature and compare it to a predefined set point. Based on this comparison, the relay activates or deactivates to control the LED strip, which serves as a heat source by converting electrical energy into warmth through its resistive material composition [16].

During winter and rainy seasons, the thermostat module maintains optimal comfort levels by initiating the heating process. Initially, if the ambient temperature falls below the set threshold of 27°C, the relay activates, causing the LED strip to emit heat. This heat permeates the chair's foam material, raising its temperature.Once the temperature reaches or exceeds 27°C, the relay deactivates, allowing the temperature to drop until it reaches 26°C. The relay then reactivates to resume the heating cycle, ensuring consistent comfort.

Conversely, during the summer season, the thermostat module operates in cooling mode to alleviate heat discomfort. Initially, when the ambient temperature reaches or exceeds 27°C, the relay activates, powering a DC cooling fan to generate a stream of cold air. This airflow cools the foam, reducing its temperature. When the temperature drops to or below 26°C, the relay deactivates, allowing the temperature to rise until it reaches 27°C. The relay then reactivates to sustain the cooling process, maintaining a comfortable seating temperature

.

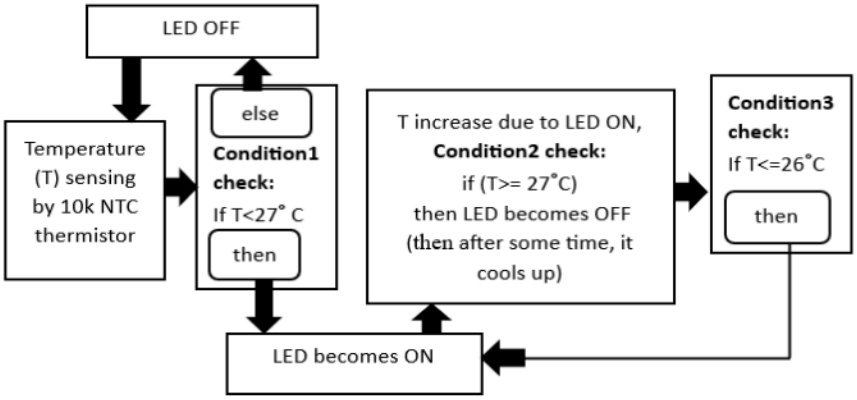

Figure 4 Warming system working

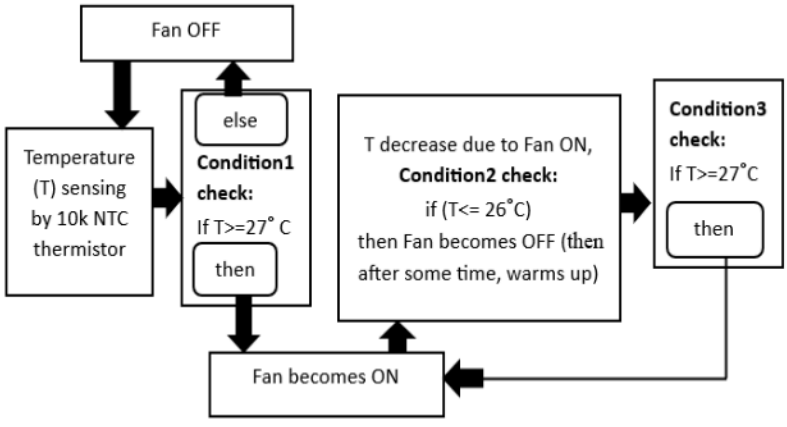

Figure 5 Cooling system working

This cyclic process continues until the power supply to the module is terminated, ensuring continuous temperature regulation adapted to seasonal conditions. Detailed operational diagrams are provided in Figure 4 and 5, illustrating the complete functionality of the warming and cooling features, respectively.

2.2.3 Remote control mobility

This feature controls the mobility of the chair using a joystick. The joystick provides analog input signals representing movement along the X and Y axes, which are transmitted to the microcontroller [17]. These analog signals are converted to digital data using the Arduino Uno's 10-bit ADC, as described by Equation 4:

$$Digital_{value} = \left(\frac{Analog\_voltage}{V_{ref}}\right) * 1023 \quad (4)$$

Upon receiving the joystick input, the microcontroller interprets the digital data to determine the joystick's precise position. This positional information is used to activate the motor driver module. The L298N motor driver, incorporating an H-Bridge circuit, manages the current flow to the BO motors, dictating the chair's movement in response to joystick manipulation [18]. Forward or backward movement along the Y-axis corresponds to forward or backward chair motion, while movement along the X-axis dictates side-to-side motion.

The H-Bridge circuit regulates motor rotation direction by selectively enabling or disabling switches based on the desired movement. When all switches (Out1, Out2, Out3, and Out4) are open, no current flows, resulting in a motor halt. For forward motion, switches Out1 and Out3 are set to HIGH, while Out2 and Out4 remain LOW. For reverse movement, Out1 and Out3 are LOW, and Out2 and Out4 are HIGH. For leftward motion, Out1, Out2, and Out4 are LOW, and Out3 is HIGH. Conversely, for rightward motion, Out2, Out3, and Out4 are LOW, and Out1 is HIGH.

$$output = (input - in_{min}) * \left(\frac{out_{max} - out_{min}}{in_{max} - in_{min}}\right) + out_{min} \quad (5)$$

Where:

- input = Y-axis joystick value
- in_min = Minimum Y-axis joystick value (0)
- in_max = Maximum Y-axis joystick value (1023)
- out_min = Minimum motor speed (-255 for backward)
- out_max = Maximum motor speed (255 for forward)

The microcontroller maps the digital values of the X and Y axes to determine the direction and speed of the motors. If the X-axis digital value is less than 512, it signifies left direction; if greater than or equal to 512, it signifies right direction. For the Y-axis, a value of 0 indicates backward movement, while 1023 indicates forward movement.

Motor speed is adjusted based on the mapped direction and the Y-axis digital value derived from Equation 5. Positive values for the left motor speed denote forward movement, while negative values indicate backward movement. The same logic applies to the right motor speed.

This precise control mechanism, illustrated in Figure 6, ensures smooth and accurate chair movement in designated directions. Table 3 documents the observed data during testing, correlating joystick directions with the corresponding chair movements, provides a comprehensive overview of how joystick inputs translate into motor control signals, enabling nine directional movements, with analog values converted to digital bits by the microcontroller.

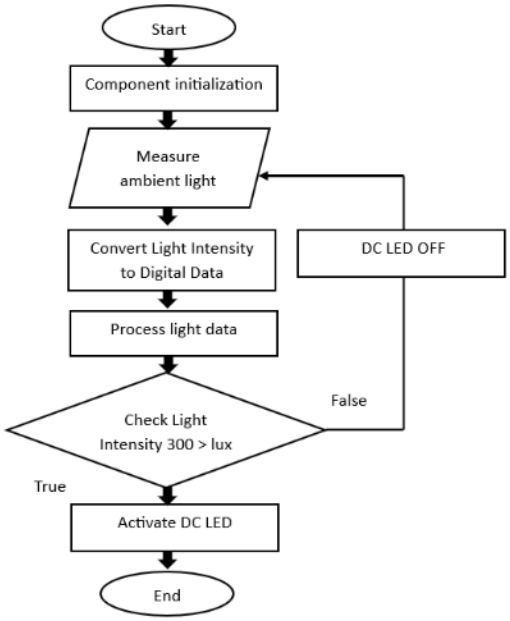

Figure 6 Working of remote-controlled mobility system

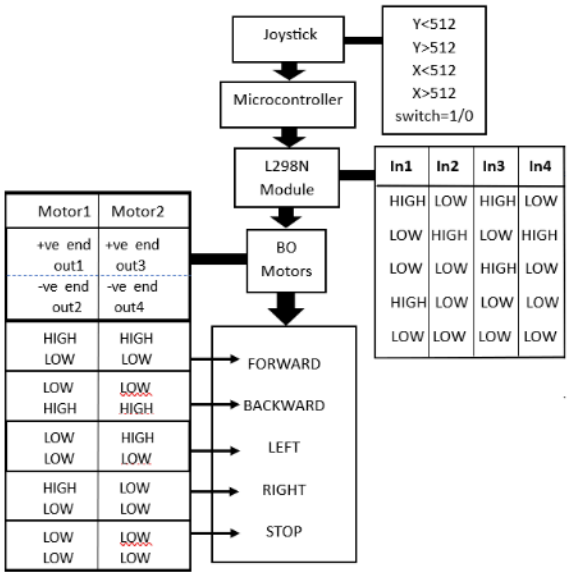

Figure 7. Workflow of Automatic lighting

Table 3. Joystick directional inputs and corresponding motor control signals

Joystick direction	Analog value (X, Y) in volts	Digital value (X, Y)	Mapped X axis (direction)	Mapped Y axis (motor direction)	Left motor speed	Right motor speed	Vehicle moving direction
Center	(2.5V, 2.5V)	(512, 512)	-	0	0	0	stop
Full left	(0V, 2.5V)	(0, 512)	Left	-	-200	200	Left
Full right	(5V, 2.5V)	(1023, 512)	Right	-	200	-200	Right
Full up	(2.5V, 0V)	(512, 0)	-	-255	-255	-255	Backward
Full down	(2.5V, 5V)	(512, 1023)	-	255	255	255	Forward
Up left	(0V, 0V)	(0, 0)	Left	-255	-255	-200	Backward-left
Upright	(5V, 0V)	(1023, 0)	Right	-255	-200	-255	Backward-right
Down left	(0V, 5V)	(0, 1023)	Left	255	200	255	Forward-left
Downright	(5V, 5V)	(1023, 1023)	Right	255	255	200	Forward-right

2.2.4 Automatic lighting

In this, the BH1750 light intensity sensor is employed to measure ambient luminosity [19]. As sensor's photodiode detects incident light, creating electron-hole pairs within the PN junction through the internal photoelectric effect.This generates an electrical signal proportional to the light intensity, which is subsequently converted into voltage by an integrated operational amplifier (OP-AMP). Working procedure is mentioned in Figure 7.

The built-in Analog-to-Digital Converter (ADC) then transforms this voltage into 16-bit digital data representing luminance in Lux. The sensor's internal logic unit processes and outputs the digital Lux data via I2C communication, with a 320kHz internal clock oscillator providing the timing reference [20]. If the measured lux value is below 300, the relay module's Common (COM) terminal connects to the Normally Open (NO) terminal, activating a DC LED. Conversely, if the lux value exceeds 300, the COM terminal connects to the Normally Closed (NC) terminal, turning off the DC LED [21]. This mechanism enables automated lighting adjustments based on ambient brightness, ensuring optimal illumination for user comfort and convenience.

2.3 Architecture

This section provides an architectural overview of the Temperature Controlled Comfortable Chair (TCCC), highlighting the integration of various system components as depicted in Figure 8, 9.

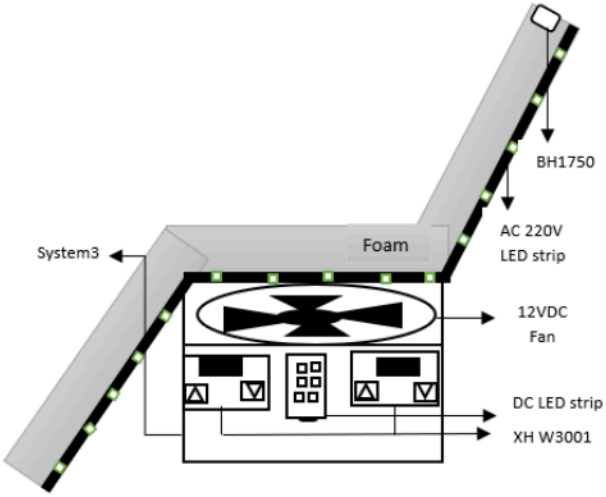

Figure 8. Placement of temperature regulation components on TCCC

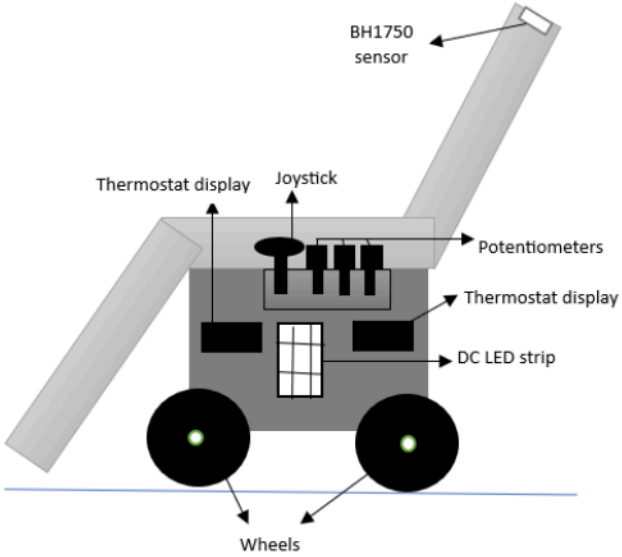

Figure 9. Placement of Automatic lighting and seat configuration modules on TCCC (outer appearance)

Figure 8 illustrates the warming and cooling system's module in chair. Positioned beneath the seat, the 220V AC LED strip provides warmth to the foam, while a DC cooling fan directs airflow upwards from a ventilated box. Two thermostats regulate this system, ensuring optimal temperature control. An external DC LED strip on the box's surface ensures uniform illumination. The BH1750 light sensor, crucial for ambient light detection, is mounted atop the chair. In Figure 9 shows the placement of components that include the servo motor control system, potentiometers, automatic lighting with a relay module, BH1750 sensor, and external DC LED strip. Potentiometers are placed near the hand position, facilitating user control, while the light sensor and LED strip are strategically positioned for efficient operation.

RESULT

This section presents findings from testing Automatic Lighting and temperature regulation features as detailed in Tables 4 and 5. Table 4 evaluated lighting conditions with a set threshold of 300 lux, where the DC LED was deactivated when ambient light exceeded this level. In low-light environments like very dark settings (41 lux) and indoor dim conditions (258 lux), the LED provided necessary illumination. Conversely, at higher indoor light levels (357 lux), the LED automatically switched off to conserve energy. Outdoors under dim light (5076 lux) and on cloudy days (10601 lux), the LED remained off, effectively utilizing natural light.

Table 4 Light intensity and LED status

Environmental condition	Measured lux values	DC LED status
Very Dark	41	ON
Dim (at home)	258	ON
Dim (at home)	357	OFF
Dim (below open sky)	5076	OFF

Cloudy (below open sky)	10601	OFF

This responsive strategy optimizes energy consumption by activating the DC LED only when necessary, ensuring sufficient lighting while supporting sustainable energy practices and addressing concerns such as Nyctophobia. Figure 10 shows the graph of illuminance (lux) versus time (seconds) as observed using the BH1750 light sensor. Under normal room conditions, the illuminance was measured at 357 lux. However, when the electricity was cut off, the illuminance dropped to 41 lux, triggering the activation of the DC light.

The temperature regulation feature was tested with minimum and maximum thresholds set at 26°C and 27°C for warming, 27°C and 26°C for cooling, respectively. Table 5 illustrates the system's adaptive response to varying seasonal and daily temperatures, aiming to maintain optimal indoor comfort while minimizing energy usage. During hot summer periods, both during the day and night, the cooling system activated when temperatures exceeded 27°C, effectively managing indoor heat levels. For instance, at 37.2°C, the cooling system engaged, with continued operation at 41.5°C and 41.7°C to maintain comfort. At night, temperatures such as 29.1°C and 28.8°C remained above the cooling threshold of 27°C, necessitating the system's continuous operation.

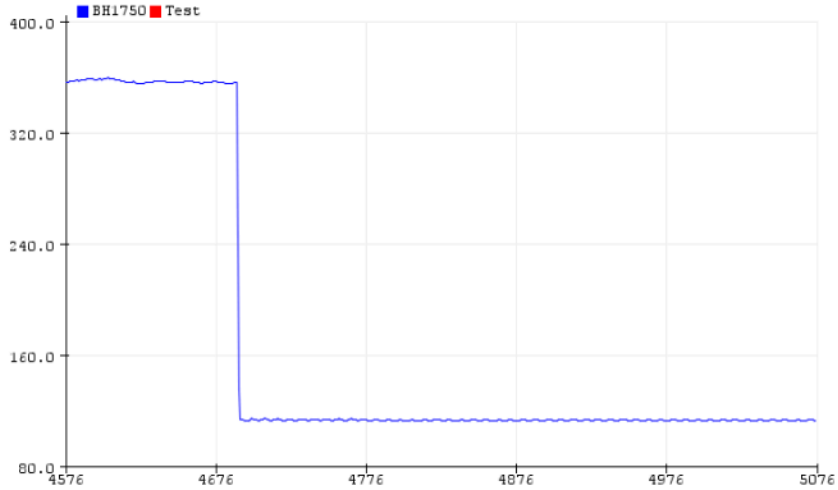

Figure 10. Illuminance vs time

In the rainy season, the warming system activated as temperatures fell below 26°C. During daytime temperatures around 21.9°C and 22.2°C, the warming system remained off since these temperatures exceeded the minimum threshold. However, at night, temperatures dropping to 19.1°C, 18.9°C, and 18.7°C activated the warming system to maintain indoor warmth. During winter days, temperatures at 27.3°C and 27.6°C exceeded the maximum warming threshold of 27°C, resulting in the deactivation of the warming system. Conversely, nighttime temperatures of 16.6°C, 16.1°C, and 15.9°C fell below the minimum threshold of 26°C, necessitating the warming system's activation to ensure comfort.

These results underscore the system's efficiency in maintaining precise climate control through adaptive responses to environmental conditions, thereby optimizing energy utilization and enhancing indoor comfort effectively.

Table 5 Seasonal temperature control status

Season	Day/Night	Measured temperature	Cooling status	Warming status
Summer	Day	37.2	ON	Deactivated
	Day	41.5	ON	
	Day	41.7	ON	
	Night	28.8	ON	
	Night	29.1	ON	
Rainy	Day	22.2	Deactivated	ON
	Day	21.9		ON
	Night	18.9		ON
	Night	18.7		ON
	Night	19.1		ON
Winter	Day	27.6	Deactivated	OFF
	Day	27.3		OFF
	Night	16.6		ON

	Night	16.1		ON
	Night	15.9		ON

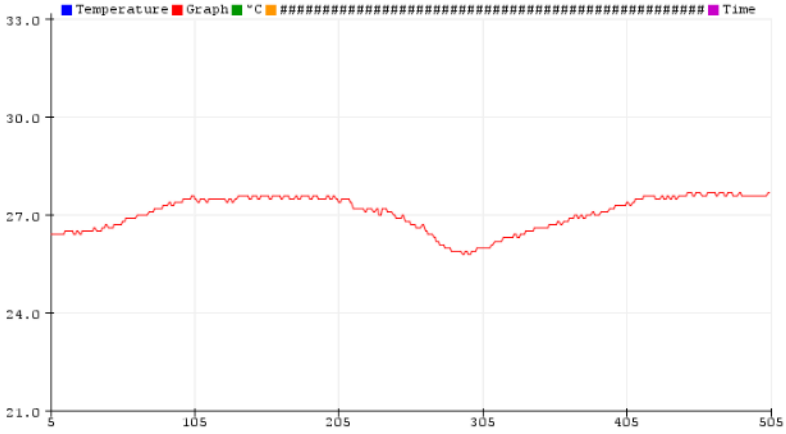

Fig. 11(a) Temperature regulation curve- warming cycle

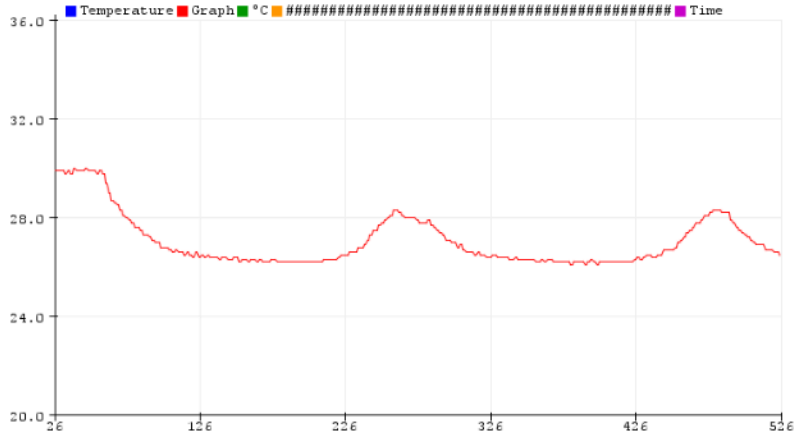

Fig. 11(b) Temperature regulation curve- cooling cycle

The temperature regulation feature effectively maintained the interior temperature within the specified range of 26-27°C. Figures 11(a) and 11(b) present the temperature regulation graphs obtained during testing. In Figure 11(a), the initial temperature reading was 26.4°C, below the maximum threshold of 27°C. The LED strip activated, providing warmth and causing the temperature to rise. Once the maximum threshold was reached, the LED strip deactivated. The temperature was stabilized for 185 seconds before a subsequent decrease was observed. The graph shows a decline in temperature until it reached the minimum threshold of 26°C, prompting the LED strip to reactivate. However, the temperature briefly continued to drop to 25.7°C due to sustained external cooling before rising again. This cyclical regulation process persisted.

In Figure 11(b), the initial temperature was 29.6°C, exceeding the maximum threshold of 27°C. The cooling fan was activated, lowering the temperature. Upon reaching the minimum threshold, the cooling fan deactivated, maintaining the cooler temperature for 120 seconds. Following this, a gradual increase in temperature was observed, with the graph showing a rise until the temperature reached the minimum threshold of 27°C, triggering the fan's reactivation. Despite this, the temperature continued to rise to 28.1°C before decreasing again due to ongoing external heat, continuing the cyclical process. Figures 11(a) and 11(b) depict temperature (°C) versus time (seconds) graphs over a total observation period of 500 seconds, ensuring optimal comfort by consistently maintaining the target temperature range.

DISCUSSION

This study aimed to develop the Temperature Controlled Comfortable Chair (TCCC), a multifunctional seating solution designed to improve comfort, mobility, and safety for individuals with diverse medical needs. The TCCC features customizable sitting and sleeping arrangements, temperature regulation, joystick-controlled mobility, and automatic lighting, targeting discomfort and pain from prolonged sitting, particularly for prehospital patients and manual wheelchair users. Results showed the TCCC's effectiveness in managing lighting and temperature. The lighting system, set at a 41lux threshold, optimized energy use while ensuring adequate illumination in low-light conditions. The temperature regulation system adjusted to various environmental conditions, with cooling activated above 27°C and warming below 26°C, maintaining a comfortable indoor climate. Despite these promising outcomes, further research is needed to address limitations. Future studies should include extensive field testing in diverse conditions to validate performance in real-world scenarios, including extreme

weather and fluctuating power supplies. Improving sensor reliability and addressing potential technical issues are crucial. Additionally, optimizing the TCCC's weight and mobility for users with severe physical limitations and confined spaces, as well as expanding features for enhanced adaptability, will further improve user experience and effectiveness.

REFERENCES

1. L. M. Aitken, J. K. Hendrikz, J. M. Dulhunty, and M. J. Rudd, "Hypothermia and associated outcomes in seriously injured trauma patients in a predominantly sub-tropical climate," Resuscitation, vol. 80, no. 2, pp. 217-223, Feb. 2009.
2. V. Hultzer, X. Xu, C. Marrao, G. Bristow, A. Chochinov, and G. G. Giesbrecht, "Pre-hospital torso-warming modalities for severe hypothermia: a comparative study using a human model," CJEM, vol. 7, no. 6, pp. 378, Nov. 2005.
3. J. LeBlanc, M. B. Ducharme, L. Pasto, and M. Thompson, "Response to thermal stress and personality," Physiol. Behav., vol. 80, no. 1, pp. 69-74, Oct. 2003.
4. N. S. Lintu, M. A. Mattila, J. A. Holopainen, M. Koivunen, and O. O. Hänninen, "Reactions to cold exposure emphasize the need for weather protection in prehospital care: an experimental study," Prehosp. Disaster Med., vol. 21, no. 5, pp. 316-320, Oct. 2006.
5. J. V. Subbarao, J. Klopfstein, and R. Turpin, "Prevalence and impact of wrist and shoulder pain in patients with spinal cord injury," J. Spinal Cord Med., vol. 18, no. 1, pp. 9-13, Jan. 1995.
6. S. Guo, R. A. Cooper, M. L. Boninger, A. Kwarciak, and B. Ammer, "Development of power wheelchair chin-operated force-sensing joystick," in Proceedings of the Second Joint 24th Annual Conference and the Annual Fall Meeting of the Biomedical Engineering Society, vol. 3, Oct. 2002, pp. 2373-2374.
7. D. Ding, R. A. Cooper, and D. Spaeth, "Optimized joystick controller," in Proceedings of the 26th Annual International Conference of the IEEE Engineering in Medicine and Biology Society, vol. 2, Sep. 2004, pp. 4881-4883.
8. P. Engel, M. Neikes, K. Bennedik, G. Hildebrandt, and F. W. Rode, "Work physiological studies performed to optimate the lever propulsion and the seat position of a lever propelled wheelchair (author's transl)," Die Rehabilitation, vol. 15, no. 4, pp. 217-228, Nov. 1976.
9. C. E. Brubaker, "Wheelchair prescription: an analysis of factors that affect mobility and performance," J. Rehabil. Res. Dev., vol. 23, no. 4, pp. 19-26, Oct. 1986.
10. L. H. Van der Woude, D. J. Veeger, R. H. Rozendal, and T. J. Sargeant, "Seat height in handrim wheelchair propulsion," J. Rehabil. Res. Dev., vol. 26, no. 4, pp. 31-50, Jan. 1989.
11. C. J. Hughes, W. H. Weimar, P. N. Sheth, and C. E. Brubaker, "Biomechanics of wheelchair propulsion as a function of seat position and user-to-chair interface," Arch. Phys. Med. Rehabil., vol. 73, no. 3, pp. 263-269, Mar. 1992.
12. S. Srivastava, M. Chandra, and G. Sahoo, "Speaker identification and its application in automobile industry for automatic seat adjustment," Microsyst. Technol., vol. 25, pp. 2339-2347, Jun. 2019.
13. S. Shulhan, F. Astwensa, F. R. Fauzan, and I. Bukhori, "Robotic arm using servo motor and Arduino Uno controlled with potentiometer," J. Electr. Electron. Eng., vol. 3, no. 2, Apr. 2021.
14. T. Amosun and W. O. Adedeji, "Design of a PLC based temperature-controlled system," REM J. Rekayasa Energi Manufaktur, vol. 8, no. 2, pp. 93-100, Nov. 2023.
15. S. F. Perdana, "AC 220V digital thermostat based drying oven XH-W3001 to improve temperature accuracy in the drying process of black betel leaves (Piper betle var nigra) at PT. FBION Karanganyar," International Conference on Early Childhood Education Multiperspectives, Aug. 2023, pp. 395-406.
16. X. Luo, R. Hu, S. Liu, and K. Wang, "Heat and fluid flow in high-power LED packaging and applications," Prog. Energy Combust. Sci., vol. 56, pp. 1-32, Sep. 2016.
17. T. Saharia, J. Bauri, and C. Bhagabati, "Joystick controlled wheelchair," International Research Journal of Engineering and Technology, vol. 4, no. 7, pp. 235-237, Jul. 2017.
18. S. Kivrak, M. Z. Erel, Y. Yalman, and K. C. Bayindir, "Design and implementation of the three-phase H-bridge motor drive controlled by two DC motors using PID controller," MECHANIKA, 2017.
19. S. N. Patrialova, T. Agasta, and I. N. Sari, "Prototype design of automatic light intensity control in smart greenhouse," International Conference on Advanced Mechatronics, Intelligent Manufacturing, and Industrial Automation (ICAMIMIA), Dec. 2021, pp. 41-46.
20. H. S. Sahu, N. Himanish, K. K. Hiran, and J. Leha, "Design of automatic lighting system based on intensity of sunlight using BH-1750," International Conference on Computing, Communication, and Green Engineering (CCGE), Sep. 2021, pp. 1-6.
21. J. W. Simatupang, L. M. Andrian, W. Zhuang, and H. Prasetyo, "A prototype of an Arduino-based protection system to overcome voltage fluctuations," International Conference on Computer, Control, Informatics, and Applications (IC3INA), Oct. 2019, pp. 172-176.
22. BEMSQIN: Design of an Efficient Hybrid Bioinspired Encryption Model for Enhancing Security of QoS-aware IoT NetworksChaudhari, D., Bamane, K.D. Kumaraguru, S., Patankar, A.J., Frontiers in Health Informatics 2024, 13(3), pp. 8676–8692